Original articles

Global sensitivity analysis of fuel-type-dependent input variables of a simplified physical fire spread model

M.I. Asensio-Sevilla[a,b,*], M.T. Santos-Martín[a,c], D. Álvarez-León[b], L. Ferragut-Canals[a,b]

[a] *University Institute of Fundamental Physics and Mathematics, University of Salamanca, Plaza de la Merced 1-4, 37008, Salamanca, Spain*
[b] *Applied Mathematics Department, University of Salamanca, Casas del Parque 2, 37008 Salamanca, Spain*
[c] *Statistics Department, University of Salamanca, Science Faculty, 37008, Salamanca, Spain*

Abstract

A new global sensitivity analysis has been conducted of fuel-type-dependent input variables of the simplified physical fire spread model (PhyFire) to understand how the use of spatial averages, that is, fuel models, influences the results of PhyFire with a view to enhancing its understanding and improving its design. The model's simplicity, the numerical techniques used, and a recent code optimisation, allow undertaking the analysis with very competitive computational times. The fuel data used correspond to grasslands, shrublands and forest in the Spanish region of Galicia. The analysis results validate the flame length sub-model proposed in the paper, which significantly improves the model's efficiency.
ⓒ 2020 International Association for Mathematics and Computers in Simulation (IMACS). Published by Elsevier B.V. All rights reserved.

Keywords: Global sensitivity analysis; Simplified physical model; Wildland fire model; Flame length model; Real wildland fire simulation

1. Introduction

Wildland fires are a clearly growing problem throughout the world, and climate change, with higher temperatures and drier terrains, increases the threat [13]. Broadly speaking, we can expect larger and more severe wildfires in the future as fire regimes change in step with climate conditions (see [3] and its references), causing extensive environmental, economic and social damage.

The scientific community has been combatting this hazard for decades, gradually making inroads in wildfire modelling. The aim of a wildfire model is to use fuel, terrain, weather conditions, ignition and fire suppression as input data to predict the spread of a fire in less than real-time, as a useful tool for firefighters. These models can be an efficient aid not only in wildfire management, but also in risk mapping, reforestation policies, resource optimisation, the issue of alerts, evacuation plans, etc.

Furthermore, improved spatial information technology (e.g., sensor monitoring, Geographic Information Systems (GIS), and satellite imagery), increased computational capabilities (parallel computing), and the development of communication technology allow the early detection of any fire, and also forecast its dynamics and spread.

---

* Corresponding author at: University Institute of Fundamental Physics and Mathematics, University of Salamanca, Plaza de la Merced 1-4, 37008, Salamanca, Spain.

E-mail addresses: mas@usal.es (M.I. Asensio-Sevilla), maysam@usal.es (M.T. Santos-Martín), daalle@usal.es (D. Álvarez-León), ferragut@usal.es (L. Ferragut-Canals).

Thanks to these technological advances, recent years have witnessed an increasing development and use of wildfire spread models [20,31–33], whose performance should seek to strike a balance between accuracy and fast execution. Nevertheless, all computational models, even the more accurate ones, can capture only a select fraction of the significant mechanisms in the wildfire process. However, the latest communication technology provides actual real-time data, which when dynamically incorporated into the simulation process make the prediction more accurate [16,17]. Furthermore, most of these models have been integrated into a GIS, providing complete tools for the prediction of wildfire spread. Most of these GIS-integrated wildfire spread models are based upon BEHAVE [2], relying on Rothermel's model [24], such as FARSITE [11], Prometheus [35], FIREMAP [36], or the coupled Weather Research and Forecasting model (WRF) and the fire-spread model, which combines the WRF atmosphere model and the SFIRE fire spread model [15], among others. The simplicity of these models provides computational efficiency, but their applicability is limited to the areas used in their calibration test. In contrast to these tools based on quasi-empirical models, the complexity and high computational cost of physical or semi-physical models have hampered the development of an efficient tool based upon them, although they do provide insight into the mechanisms that drive wildfire spread. The rapid increase in computing power allows more complex models to be a real option, so research is focusing on physical-based models.

These premises have led the authors to review their PhyFire simplified physical model (previously called PhFFS-Physical Forest Fires Spread) [21] in order to include the necessary improvements that have emerged as new real examples are simulated with the model. The PhyFire model is a simplified physical model based on the fundamental physics of combustion and fire spread. The resulting Partial Differential Equations are solved using efficient numerical and computational tools to obtain a software with efficient levels comparable to empirical models. At present, the current PhyFire model is integrated into a GIS for use in Spain [22], and is available through the url: http://sinumcc.usal.es.

The PhyFire model depends on several input variables and three model parameters. An initial model validation was carried out in [21] through a global sensitivity analysis (GSA) of the input factors, including fuel-dependent input variables and model parameters. This analysis has enabled us to determine which input factors and parameters are the most influential on model outputs as a first step in the difficult process of model parameter adjustment. It also supports the conclusion that the PhyFire model duly reflects the importance of radiation in windless conditions and of convection under windy conditions.

Most of the PhyFire model's input variables, as in other fire spread models, are spatial-dependent. As no exhaustive spatial information on the model input variable is available, a simplified map-based approach is used. The PhyFire uses three bespoke maps [22]: topographic, fuel-load, and fuel-type. Both these fuel maps inevitably lack accuracy due to the scarcity of updated data and to the use of mean values (fuel models) that lead to biased outputs, reducing the model's reliability.

This paper proposes a new GSA for discovering which fuel-type-dependent input variables most influence the model's output, namely, the rate of spread, with a view to understanding how the use of spatial averages, that is, fuel models, influence the results of PhyFire model simulations. The major influence of one of these input variables, flame length F, has informed our flame length sub-model depending on wind speed and the slope of the terrain in all the proposed scenarios (different wind conditions and slopes).

Any GSA involves repeatedly running the model (i.e., solving the model equations), and so an efficient numerical solution is required. The numerical solution proposed [21] for the model equations seeks to reduce the computational time by defining the active nodes and using parallel computation. In addition, the code has been optimised in this new paper, and all the computer calculations have been performed on the hardware at Supercomputing Castilla and León (SCAYLE), to take full advantage of its computing technologies.

The data and information used for the examples analysed in this study involve grasslands, shrublands and forest in Galicia, Spain, based on an extensive survey [4].

The outline of the paper is as follows. In the first part of Section 2.1, we briefly summarise the PhyFire model equations, focusing on the fuel-type-dependent input variables, which will be analysed; we then outline certain general aspects about GSA, and we end this section with a detailed description of the experiments. Section 3, presents the results of the experiments and the flame length sub-model derived. We add a real application of both models, the original PhyFire, and the improved model with the flame length sub-model, to the same wildfire in an area of Galicia. Finally, some conclusions are provided in Section 5.

2. Methodology

2.1. A brief summary of the PhyFire model

This section describes the mathematical equations corresponding to the *Physical Forest Fire Spread* model (PhyFire) developed by the authors. This description, focuses on the model's fuel-type-dependent input variables guided by the targets set out here. For a more detailed explanation of the model, its development, numerical solution and applications, see [8,21,22] and its references.

The non-dimensional equations governing the current version of the PhyFire model are:

$$\partial_t e + \beta \mathbf{v} \cdot \nabla e + \alpha u = r \quad \text{in } S \quad t \in (0, t_{max}), \tag{1}$$

$$e \in G(u) \quad \text{in } S \quad t \in (0, t_{max}), \tag{2}$$

$$\partial_t c = -g(u)c \quad \text{in } S \quad t \in (0, t_{max}). \tag{3}$$

Surface S is large enough to ensure the fire does not reach the boundary during the time of study $(0, t_{max})$, so homogeneous Dirichlet boundary conditions can be considered. We complete the model with appropriate initial conditions representing the location of the fire ignition point or intermediate fire perimeter, and the initial distribution of fuel, including any possible firebreaks. Surface S is defined by a mapping $(x, y) \longmapsto (x, y, h(x, y))$ representing the height of the surface S.

The unknowns are the following bidimensional variables defined in $S \times (0, t_{max})$: $e = \frac{E}{MCT_\infty}$, dimensionless enthalpy, $u = \frac{T - T_\infty}{T_\infty}$, the dimensionless temperature of the solid fuel and $c = \frac{M}{M_0}$, and the mass fraction of solid fuel. See [21] for a detailed explanation of all the physical magnitudes and parameters of Eqs. (1)–(3).

PhyFire depends on three unknown parameters which must be adjusted in each case. First, the natural convection coefficient H $(\text{J s}^{-1} \text{ m}^{-2} \text{ K}^{-1})$, which appears in the zero-order term αu in the partial differential equation (1), where $\alpha = \frac{H[t]}{MC}$. Second, the correction factor β of convective term $\beta \mathbf{v} \cdot \nabla e$ in Eq. (1). Third, the mean absorption coefficient a that appears in the total radiation intensity differential equation to be solved in order to compute the term r in Eq. (1) representing the radiation from the flames above the surface where the fire is burning (see [21]).

On the other hand, a fire's evolution is strongly affected by some of the input variables, such as wind and slope, the ambient temperature, and fuel load, which are represented, respectively, in the PhyFire through the non-dimensional wind velocity $\mathbf{v}$, the height h of the surface S, the fuel load M, and the reference temperature T_∞. All of them are relatively easy to measure and define different scenarios.

Finally, there are other input variables that depend on each type of fuel, some of which are not so easy to measure: heat capacity C, pyrolysis temperature T_p, flame temperature T_f, combustion half-life $t_{1/2}$, maximum fuel load M_0, fuel moisture content M_v, and flame length F.

All the model parameters and input variables are listed in Table 1 and explained in detail in [21], including a previous GSA of the PhyFire model's input variables and model parameters. This initial analysis has enabled the authors to conclude that the most relevant parameter in terms of the rate of spread and fire thickness in low wind conditions is the mean absorption coefficient a of the radiation term, which is consistent with the importance of radiation in low wind fires. This analysis has also reflected the major role of convection in fires driven by high winds through the importance that the correction factor of convective term β has in the GSA of windy examples. As mentioned earlier, the aim here is to focus the GSA on the fuel-type-dependent input variables for different scenarios to analyse whether the use of mean values through wide areas with some internal variability (fuel models) significantly affects the outputs. As will be seen in due course, the results of this new global sensitivity analysis reveal a strong influence of one of these fuel-type-dependent input variables, flame length F, in all the proposed scenarios (different wind conditions and slopes), whereby the PhyFire model can be improved through a flame length sub-model depending on wind speed and the slope of the land. Flame length F appears in the radiation term r in Eq. (1).

Any GSA involves a large number of simulations, with the resulting computational cost, so the efficiency of the numerical and computational techniques used is crucial. We use a $P1$ finite element approximation on a regular mesh for spatial discretisation and a Crank–Nicolson finite difference scheme time discretisation of the total derivative for Eqs. (1)–(3). All the linear terms remain implicit, and a fixed-point iteration is proposed to solve the non-local radiation term r that heavily depends on the temperature u and on fuel mass c. Details of this numerical scheme can be found in [21]. The maximal monotone property of the multivalued operator in Eq. (2) allows using duality

Table 1
PhFFS parameters and input variables.

Fuel-type-dependent input variables	Symbol	Units
Heat capacity	C	J K^{-1} kg^{-1}
Pyrolysis temperature	T_p	K
Flame temperature	T_f	K
Combustion half-life time	$t_{1/2}$	s
Maximum fuel load	M_0	(kg m^{-2})
Moisture content	M_v	kg of water/kg of dry fuel
Flame length	F	m
Input variables defining scenarios	**Symbol**	**Units**
Non-dimensional wind velocity	$\mathbf{v}$	–
Height of the surface	h	m
Reference temperature	T_∞	K
Fuel load	M	kg/m^2
Model parameters	**Symbol**	**Units**
Mean absorption coefficient	a	m^{-1}
Natural convection coefficient	H	J s^{-1} m^{-2} K^{-1}
Correction factor of convective term	β	–

methods for its numerical solution [6]. We consider an exact perturbation of the multivalued operator, and the properties of this perturbed operator, with an appropriate choice of the parameters, allow defining the resolvent, as well as its Yosida approximation, whereby the new nonlinear univalued operator equivalent to the multivalued one can be solved by a fixed-point iteration. For further details of how to numerically treat this multivalued operator, see [9]. We should describe certain aspects of the numerical computation of the radiation term. Because radiation essentially comes from the flames, our PhyFire model considers that the gases produced by pyrolysis burn above the fuel layer, producing a flame over that layer that emits radiation, reaching the points ahead of it, heating the surrounding non-burned fuel, and thus allowing the fire to propagate. We reduce the computational cost by computing the *radiation matrix* once out of the time loop, which represents the nodes of the finite element mesh reached by the radiation emitted by each node. In practice, only the terms in the neighbourhood of the flame are calculated, denoted as the set of *active nodes* for each time step [8], thus reducing the computational cost. The PhyFire model was developed under C++, using Neptuno++, a finite element toolbox mainly developed by L. Ferragut [7], and has the advantages of the parallel paradigm using OpenMP API. In addition, the code has recently been optimised.

2.2. The global sensitivity analysis

A sensitivity analysis is required to reflect each input factor's importance on the values of a mathematical model's output variable. This is crucial when the input factors are affected by uncertainties, and fire propagation models are a good example of this situation. A GSA generally pursues one of these four objectives: screening or factor fixing, ranking or factor prioritisation, variance cutting for risk assessment, and factor mapping to support robust decision-making. The aim of the GSA developed here is the ranking or factor prioritisation typically used to enhance model understanding [28]. There are many ways to conduct such analyses [12], but in this paper, as in [21], we have opted for a GSA [25,26] based on the decomposition of the variance of the output in a unique additive series of the variance of independent functions of increasing dimensionality. Variance-based methods are suitable for application to a limited number of input variables, as in the case here [14]. All the input parameters in this analysis are varied simultaneously over the entire parameter space, which allows evaluating each input factor's contributions and the interactions between factors in the model's output variance.

This decomposition assigns each input factor's effect on the model output uncertainty through the variances of the main effects, and of any group of input factors through higher-order variances (interaction effects).

Variance-based methods calculate two indices, with the first-order index (S_i) measuring the average influence of an input factor (X_i) to the total variance on the model output ($V[Y]$), without the interaction effects for this factor.

Total indices (S_{T_i}) calculate the sum of the factorial indices involving each factor,

$$S_i = \frac{V[E[Y|X_i]]}{V[Y]}$$

$$S_{T_i} = \frac{E[V[Y|X_{\sim i}]]}{V[Y]}$$

where $V[E[Y|X_i]]$ is the amount of expected variance due to the main effect that would be removed from the total variance $V[Y]$ if the true value of factor X_i could be determined, and $E[V[Y|X_{\sim i}]]$ is the contribution to the variance conditioning regarding all the factors except X_i.

The GSA studies the uncertainty of the output variable through the uncertainty of the input factor by estimating the probability density functions (PDFs) for each input variable.

Two of the most widely used methods are the Extended Fourier Amplitude Sensitivity Test (FAST) [27] and the Sobol method [30], which these authors have already used in a previous analysis of the PhyFire model in [21]. Both methods use variance decomposition techniques to provide a quantitative measure of the importance of the input to the output variance. The main difference between FAST and the Sobol method is the underlying algorithm in the multidimensional integration of the sensitivity indices (Monte Carlo integration method for Sobol).

Both methods are integrated in the SimLab program [29], and we have tested them with similar results. The Sobol method (with respect to FAST) does not use the transformation function to generate the combinations of factors, and requires each factor's statistical distribution as input. For reasons of simplicity, this paper shows only the results for the Sobol sensitivity analysis that determine each input parameter's contribution and their interactions with the overall model's output variance. Extended FAST sensitivity analysis provides very similar results.

GSAs are generally sampling-based methods, so a critical step is the choice of sample size to run the simulations, whereby samples that are too small may not provide robust results, and the computational cost for very large sample sizes may become too high, especially for complex models, as in environmental applications. In [28], an attempt is made to establish criteria to assess different types of convergences of GSA results, giving typical convergence values involving the number of model evaluations (sample size N) in terms of the number of input factors, the GSA's objective, and the GSA method. In this study, where a variance-based sensitivity analysis (Sobol and FAST) is performed for ordering the input factors (ranking), with seven or nine input factors, a sample size $N \approx 10^4$ ensures robust results (see Fig. 1 in [28]). There are other methods that require fewer number of model evaluations, such as the adaptative ANOVA decomposition [37], or the derivative-based GSA [14]. Following the methodology of the previous work [21], we have opted for a variance-based method and a large sample, reducing the operational cost by optimising the model code and using massive parallel architectures. A secondary outcome here, which exceeds this paper's aims, is the model code's adaptation to parallel architectures to improve its efficiency for real-case simulations, albeit with a higher computational cost.

2.3. Experimental

The data required for this study were taken from [4], which contains detailed measurements for the main forestry fuels in Galicia, in northwest Spain. These data provide valuable information on these fuels' main physical features related to their fire behaviour. The data cover four types of grasslands, 56 types of shrublands, and 83 types of tree, including pines, eucalyptus and other deciduous species, all of which are very common in Galicia and of major importance from the perspective of forest fire protection. [4] includes forecasting data on flame length in several wind and slope scenarios that are of particular interest to this study.

Estimates of the PDFs of the seven fuel-type-dependent input variables analysed were derived from data in [4] and other scientific papers as necessary. All the relevant features of the fuel-type-dependent input variables and the corresponding PDFs are summarised in Table 2. The PDFs have been fitted with the Kolmogorov–Smirnov tests.

The spatial domain for the experiments has a manageable but realistic scale, namely, $5000 \, \text{m} \times 1000 \, \text{m}$, which ensures a low computational cost for each model evaluation. The fire front is located at a distance of 500 m from the short side of less height. Three different slopes, $0°$, $20°$ and $40°$, have been used to fit the data included in [4], together with three wind velocities: $10 \, \text{km h}^{-1}$, $20 \, \text{km h}^{-1}$ and $30 \, \text{km h}^{-1}$. Both factors are taken in the same direction; that is, the fire front follows both the slope and the wind.

The analysis's output variable, the rate of spread (ROS), is computed as the slope of the linear regression line used to fit the position of the fire front at each moment of the simulation, measured from a point at a distance

Table 2
Fuel-type-dependent input variables.

Variable	PDF	Source of information
C	N(1700, 133)	[23]
T_p	N(575, 25)	[19]
T_f	T(1000, 1400, 1175)	[1]
$t_{1/2}$	U(100, 400)	[5]
M_v	U(0, 30)	[4]
M_0	U(1.091, 5.339)	[4]
F	N(6.03, 2.297)	[4]

of 1000 m from the fire ignition up to 300 m to the end of the domain, in the half lengthwise, in order to avoid distortion due to initial and boundary conditions.

The GSA was conducted for the seven fuel-type-dependent input variables in Table 2, with a sample size of $N = 8,192$ for the Sobol to ensure a good estimation of the sensitivity indices [25,26], using SimLab software (version 2.2) for sensitivity analysis, whose structured design is based on quasi-random sampling, [29,34]. The analysis was conducted for each one of the nine scenarios described before, and for the following values of the model parameters: natural convection coefficient $H = 5$, correction factor of convective term $\beta = 0.01$, and two different values for the mean absorption coefficient: $a = 0.5$ and $a = 0.25$. Although a single value for the mean absorption coefficient was selected initially, we repeated the analysis for a second lower value to confirm the conclusions obtained. All the parameter values selected correspond to the orders of magnitude obtained in the parameter adjustment of the PhyFire model developed in [21].

To obtain the experimental results within a reasonable time, the model was run at the Supercomputer Cluster at the Supercomputing Center in the Spanish region of Castilla y Leon (managed by SCAYLE). This cluster was built using 114 Supermicro nodes with Haswell architecture. Each node contains two processors: Intel Xeon E5-2630 v3 (eight cores @ 2.40 GHz) and 32 GB RAM (ratio 2 GB/core), and the node interconnection involves InfiniBand/Gigabit Ethernet. The theoretical peak performance of the fully operational system is ≈ 131.8 TFLOPS.

3. Results

Fuel length F is the most influential fuel-type input parameter for each one of the nine scenarios, thereby revealing a clear weakness in the PhyFire model. Fig. 1 depicts the first-order sensitivity indices (black bars) and the total ones (grey bars) computed with the Sobol method for ROS and all the scenarios. The graphics show that flame length significantly controls the simulated front's ROS, even unexpectedly so in high wind situations. The results are similar for other values of the model parameters a, β and H, see Fig. 2, where the first-order sensitivity indices (black bars) and the total ones (grey bars) are compared for two different values of the mean absorption coefficient and an intermediate scenario (wind 20 km/h, slope 20%).

Data from [4] show that flame length clearly depends on wind strength and surface slope. This, together with the results of the sensitivity analysis, leads us to propose the following flame length sub-model,

$$F = (F_H + F_v |v|^{1/2})(1 + F_s s^2) \tag{4}$$

where, F_H is a flame length independent parameter, F_v is a wind correction factor, F_s is a slope correction factor, $|v|$ is the wind strength, and s represents the slope at each point on the surface. The first factor in Eq. (4) corresponds to the correction of flame length due to the wind. This expression is based on the observation of the experimental curves for different fuels in [4], where the increase in the length of the flame due to the wind responds to such a function. F_H corresponds to zero wind, and the correction coefficient F_v has been added to experimentally adjust the different behaviours for each type of fuel by a least-squares method. The second factor in Eq. (4) corresponds to the correction of flame length according to surface slope. When there is no wind or slope, in other words, the flame is vertical and its height is equal to its length, as deduced from [5], a relationship can be derived between flame height and the vertical gas velocity inside it. When there is a slope, the following proportionality factor appears,

$$\frac{1}{\cos^2 \alpha} = 1 + \left(\frac{\partial h}{\partial x}\right)^2 + \left(\frac{\partial h}{\partial y}\right)^2 = 1 + s^2$$
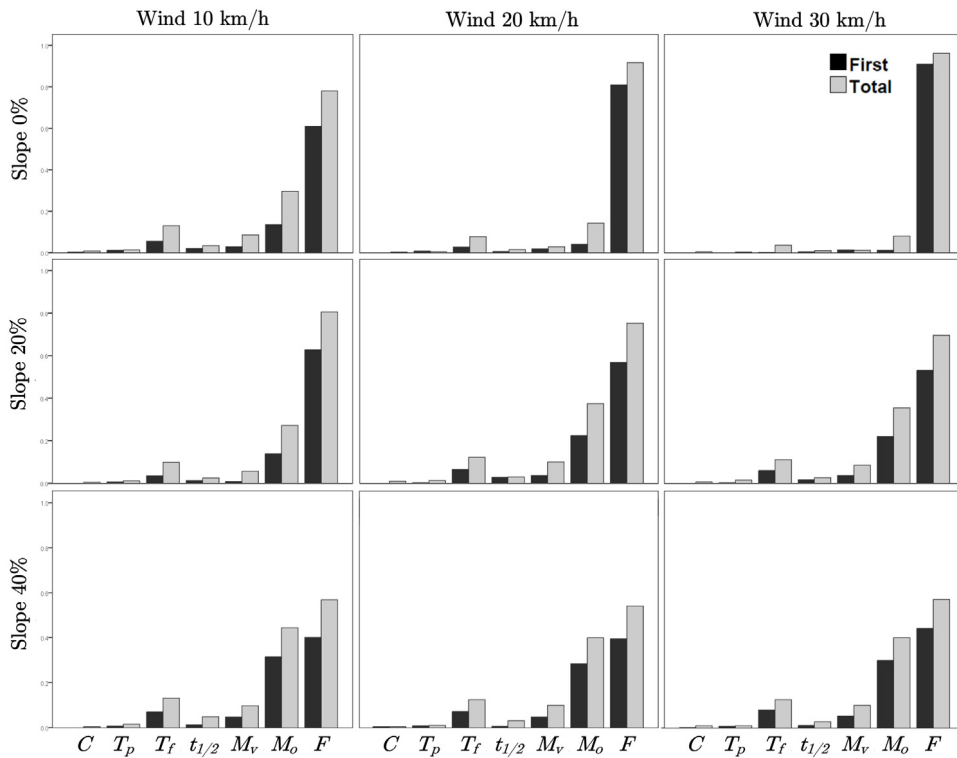
Fig. 1. Sensitivity indices obtained with the Sobol method for ROS, all scenarios and $a = 0.25$.
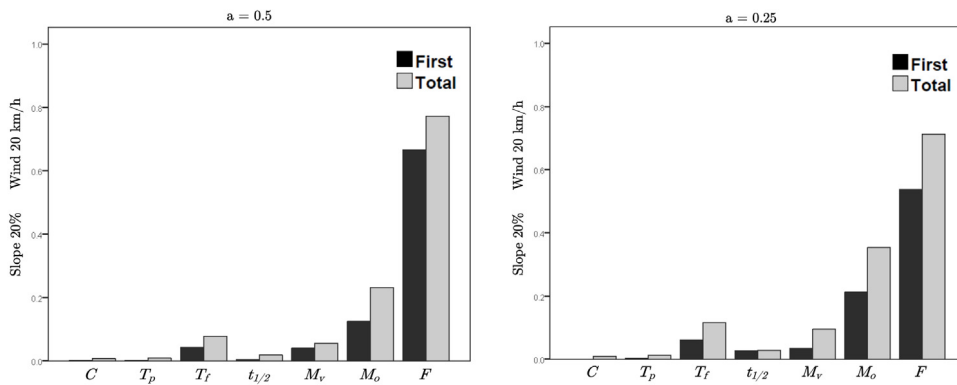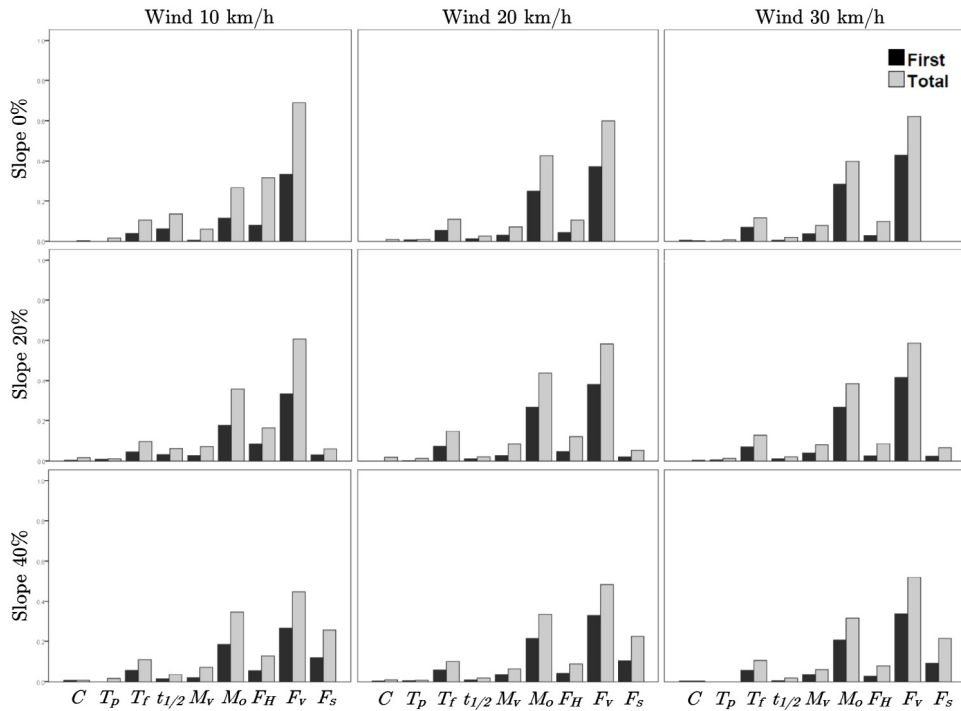

Fig. 2. Sensitivity indices obtained with the Sobol method for ROS, wind 20 km/h, slope 20%, $a = 0.5$ (left) and $a = 0.25$ (right).

where α is the angle between the horizontal plane and the plane tangential to the surface S at each point, and $h = h(x, y)$ is the surface height, so s is the slope at each point on the surface S. Again, a correction factor has been added to this expression to adjust data from [4] in the least-squares sense, the slope correction factor F_s.

The flame lengths of the fuels in [4] for different scenarios (wind and slope) have been measured and adjusted by least squares to Eq. (4), and a sample of the three variables F_h, F_v and F_s, has been obtained. SPSS software provides the Kolmogorov–Smirnov test, with Lilliefors correction for normality, under the null hypothesis that the data come from a specific distribution. The tests had a p-value over 0.05, indicating that the data fit the distributions shown in Table 3.

Table 3
Fuel-type-dependent input variables.

Variable	PDF	Source of information
F_H	U(0.1262, 1.4518)	[4]
F_v	N(0.57, 0.27)	[4]
F_s	N(2.51, 1.21)	[4]

Fig. 3. Sensitivity indices obtained for the new model with the Sobol method for the ROS, all scenarios and $a = 0.25$.

Another GSA has been performed for the new set of fuel-type-dependent input variables, C, T_p, T_f, $t_{1/2}$, M_v and M_0, with the PDFs described in Table 2, and F_H, F_v, and F_s with the PDFs described in Table 3, with a sample size of $N = 10,240$ for the Sobol method.

Fig. 3 shows the first-order sensitivity indices (black bars). The total ones (white bars) computed with the Sobol method for the ROS are represented for all the scenarios and $a = 0.25$, except for the nine fuel-type-dependent input variables analysed for the new model. The shortcomings and weaknesses detected in the previous model due to the excessive weight of the flame length are no longer present.

4. Real case in Galicia

The PhyFire model improved with the flame length sub-model is tested by simulating a real fire that occurred in Galicia (Spain), in an area covered with Pinus pinaster and different types of dormant brush, short grass and timber grass, as described in [4]. This real fire occurred in an area near Osoño, Ourense, an inland province in the south of Galicia. The fire ignited at 3.45 pm local time on 17 August 2009; and was brought under control at 11.00 pm on the same day. The fire burnt 224 ha: 185 ha of forest area and 39 ha of agricultural area. The fire's spread and its behaviour were reconstructed and documented by the coordinator of the fire-suppression operations [18], and previously simulated with the former version of PhyFire in [22], which provides specific data on topography, vegetation, weather conditions, and the fire's real evolution.

This paper simulates the initial time of this real fire, specifically four and a half hours, updating wind data (wind speed and direction) every half hour, and providing graphic results of the burnt area and fire front every 15 min. The

Table 4
Fuel-type-dependent input variable values shared by both versions of the PhyFire model.

Fuel type (Behave)	M_0	M_v	T_f	T_p	$t_{1/2}$	C
Short grass (1)	0.1	0%	1300	500	100	1800
Timber grass (2)	1.0	10%	1300	500	100	2000
Brush (5)	2.3	10%	1300	500	200	2300
Dormant brush (6)	2.2	10%	1300	500	200	2300
Inflammable brush (7)	2.4	15%	1300	500	300	2300

Table 5
Values of flame length input variables: F for the original PhyFire model, and F_H, F_v and F_s for the improved PhyFire model.

Fuel type [4]	F	F_H	F_v	F_s
Short grass (Ac-01)	2.5	0.2606	0.6001	5.4330
Timber grass (Pa-06)	4.0	1.1100	0.4712	0.6759
Brush (Eu-06)	5.5	3.7780	0.5075	2.8280
Dormant brush (Cl-02)	7.0	3.3240	0.4888	2.6880
Inflammable brush (Ea-08)	8.0	3.9320	0.6752	3.0150

Table 6
Model comparison by similarity indices.

| *Similarity index*	Sørensen	Jaccard	Kappa
PhyFire model	0.74	0.59	0.67
Improved PhyFire model	0.87	0.77	0.84

simulation area is a rectangle measuring 3315 m × 2740 m. The computing time for the original PhyFire model on a laptop equipped with an Intel Core i7-2410M processor (two cores, each one working at a frequency of 1.8 GHz) and 4 GB RAM, was 20 min and 5 s, and for the improved PhyFire model it was 12 min and 32 s. We should stress that the flame length sub-model is not the only improvement in the upgraded version of the PhyFire model, as a code optimisation system has been developed to provide shorter calculation times.

The model parameter values for this simulation are as follows: mean absorption coefficient $a = 0.095 \, \text{m}^{-1}$, natural convection coefficient $H = 15 \, \text{J s}^{-1} \, \text{m}^{-2} \, \text{K}^{-1}$, and the correction factor of convective term $\beta = 0.015$. The values of the fuel-type-dependent input variables used for the simulation are summarised in Tables 4 and 5 for each one of the five fuel types in the studied area, adapting the information from [4] to the BEHAVE classification [2]. Values of M_0 and F are obtained from [4] corresponding to the fuel types according to the fuel mapping of the area (see [22]) and data from [18]. M_v depends on the fuel type and ambient humidity reported in [18]. T_f, T_p are standard values. $t_{1/2}$ and C vary slightly depending on fuel type, but have little influence on the ROS. Finally, F_h, F_v and F_s have been adjusted in the sense of least squares to the data from [4].

In addition, three of the firebreaks the firefighting team created by widening a number of roads on the southern flank during the early hours of the fire have been added to the simulation by modifying the initial fuel data, being identified in Figs. 4 and 5 by thick red lines.

Figs. 4 and 5 compare the output of the simulations after four hours and 15 min of real time, burnt area (grey) and fire front (orange), with the real intermediate perimeter corresponding to the same period, that is, at 8.00 pm. In order to measure the accuracy of the simulations, three similarity indices have been calculated: Sørensen similarity index S, Jaccard similarity coefficient J, and Kappa coefficient K [10]. These similarity indices belong to the fields of image analysis and geospatial statistics. Values of 1 mean perfect agreement between the simulated and observed fire perimeter, while values of 0 mean no agreement. The values of these indices for both the original PhyFire and the improved PhyFire models are listed in Table 6.

Fig. 4 corresponds to the original PhyFire model; the ROS is similar to the real one, and the similarity indices in Table 6 record a substantial agreement. However, the enhanced PhyFire model, in addition to the lower computational cost, provides more reliable and accurate results, as may be observed in Fig. 5 and Table 6, where the similarity indices reveal an almost perfect agreement.
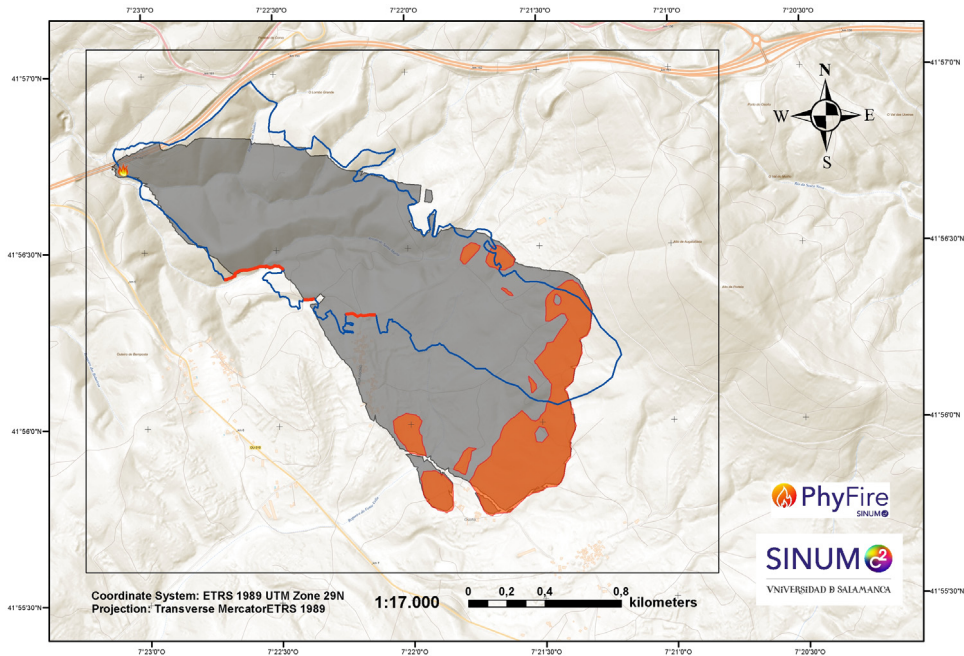
Fig. 4. Osoño fire: Burnt surface (grey area) and active front (orange area) simulated using the PhyFire model, compared to the real partial perimeter (blue line) at 8.00 pm. Thick red lines represent firebreaks, and the black square is the simulation domain. (For interpretation of the references to colour in this figure legend, the reader is referred to the web version of this article.)
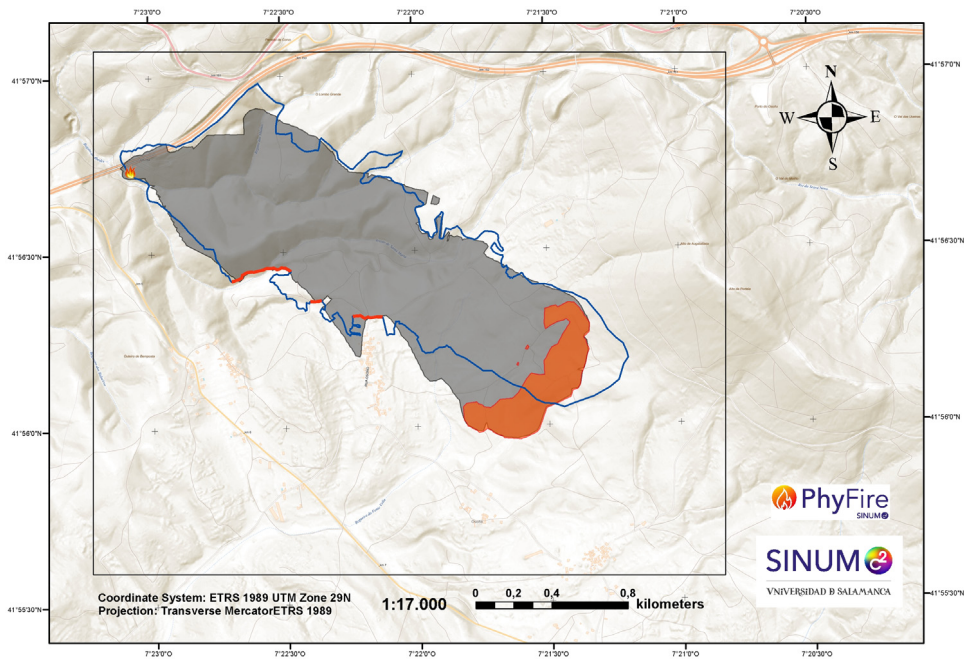
Fig. 5. Osoño fire: Burnt surface (grey area) and active front (orange area) simulated using the PhyFire model improved with the flame length sub-model, compared to the real final perimeter (blue line) at 8.00 pm. Thick red lines represent firebreaks, and the black square is the simulation domain. (For interpretation of the references to colour in this figure legend, the reader is referred to the web version of this article.)

5. Conclusions

A new global sensitivity analysis of the physical forest fire spread model PhyFire, focused on fuel-type-dependent input variables, has significantly improved its design. Experimental data show that flame length depends on wind strength and surface slope, and the results of the sensitivity analysis performed in this study confirm that the proposed flame length sub-model provides better results, overcoming the model's shortcomings. The PhyFire code has been finetuned to provide shorter calculation times, and redesigned for massively parallel architectures. Furthermore, the results have been confirmed by the simulation of a real wildfire in an area with the same kind of forestry fuel. The analysis involved forestry fuels in Galicia. The extensive review and adjustment of the flame height data of [4] will be used in future research.

Acknowledgements

References

[1] A. Àgueda, E. Pastor, Y. Pérez, E. Planas, Experimental study of the emissivity of flames resulting from the combustion of forest fuels, Int. J. Therm. Sci. 49 (3) (2010) 543–554, http://dx.doi.org/10.1016/j.ijthermalsci.2009.09.006.

[2] P. Andrews, Behave: Fire Behaviour Prediction and Fuel Modelling System - Burn Subsystem, Part 1, General Technical Report INT-194, U.S. Department of Agriculture, Forest Service, Intermountain Forest and Range Experiment Station, Ogden, UT, 1986.

[3] C. Aponte, W. de Groot, B. Wotton, Forest fires and climate change: causes, consequences and management option, Int. J. Wildland Fire 25 (2016) i–ii, http://dx.doi.org/10.1071/WFv25n8_FO.

[4] S. Arellano, J. Vega, A. Ruíz, A. Arellano, J. Álvarez, D. Vega, E. Pérez, Foto-guía de combustibles forestales de Galicia. Versión I, Andavira Editora, S.L., 2016.

[5] J. Balbi, F. Morandini, X. Silvani, J. Filippi, F. Rinieri, A physical model for wildland fires, Combust. Flame 156 (12) (2009) 2217–2230, http://dx.doi.org/10.1016/j.combustflame.2009.07.010.

[6] A. Bermúdez, C. Moreno, Duality methods for solving variational inequalities, Comput. Math. Appl. 7 (1) (1981) 43–58, http://dx.doi.org/10.1016/0898-1221(81)90006-7.

[7] J.M. Cascón, L. Ferragut, M.I. Asensio, D. Prieto, D. Álvarez, Neptuno ++: An adaptive finite element toolbox for numerical simulation of environmental problems, in: XVIII Spanish-French School Jacques-Louis Lions About Numerical Simulation in Physics and Engineering, Las Palmas de Gran Canaria, 2018.

[8] L. Ferragut, M. Asensio, J. Cascón, D. Prieto, A wildland fire physical model well suited to data assimilation, Pure Appl. Geophys. 172 (1) (2015) 121–139, http://dx.doi.org/10.1007/s00024-014-0893-9.

[9] L. Ferragut, M. Asensio, S. Monedero, A numerical method for solving convection–reaction–diffusion multivalued equations in fire spread modelling, Adv. Eng. Softw. 38 (6) (2007) 366–371, http://dx.doi.org/10.1016/j.advengsoft.2006.09.007.

[10] J. Filippi, V. Mallet, B. Nader, Representation and evaluation of wildfire propagation simulations, Int. J. Wildland Fire 23 (2014) 46–57, http://dx.doi.org/10.1071/WF12202.

[11] M. Finney, FARSITE: Fire Area Simulator–Model Development and Evaluation, Research Paper RMRS-RP-4 (revised), U.S. Department of Agriculture, Forest Service, Rocky Mountain Research Station, Ogden, UT, 2004.

[12] D.M. Hamby, A review of techniques for parameter sensitivity analysis of environmental models, Environ. Monit. Assess. 32 (2) (1994) 135–154, http://dx.doi.org/10.1007/BF00547132.

[13] W.M. Jolly, M.A. Cochrane, P.H. Freeborn, Z.A. Holden, T.J. Brown, G.J. Williamson, D.M.J.S. Bowman, Climate-induced variations in global wildfire danger from 1979 to 2013, Nature Commun. 6 (7537) (2015) http://dx.doi.org/10.1038/ncomms8537.

[14] M. Lamboni, B. Iooss, A.-L. Popelin, F. Gamboa, Derivative-based global sensitivity measures: General links with Sobol' indices and numerical tests, Math. Comput. Simulation 87 (2013) 45–54, http://dx.doi.org/10.1016/j.matcom.2013.02.002.

[15] J. Mandel, J.D. Beezley, A.K. Kochanski, Coupled atmosphere-wildland fire modeling with WRF 3.3 and SFIRE 2011, Geosci. Model Dev. 4 (3) (2011) 591–610, http://dx.doi.org/10.5194/gmd-4-591-2011.

[16] J. Mandel, J.D. Beezley, A.K. Kochanski, V.Y. Kondratenko, M. Kim, Assimilation of perimeter data and coupling with fuel moisture in a wildland fire–atmosphere {DDDAS}, Procedia Comput. Sci. 9 (2012) 1100–1109, http://dx.doi.org/10.1016/j.procs.2012.04.119.

[17] J. Mandel, L.S. Bennethum, J.D. Beezley, J.L. Coen, C.C. Douglas, M. Kim, A. Vodacek, A wildland fire model with data assimilation, Math. Comput. Simulation 79 (3) (2008) 584–606, http://dx.doi.org/10.1016/j.matcom.2008.03.015.

[18] A. Morillo, Análisis del comportamiento del fuego forestal observado y simulado: estudio del caso del incendio forestal de Osoño (Vilardevós)-Verín-Ourens (Master's thesis), Higher Polytechnical School of Lugo, University of Santiago de Compostela, 2011, (in Spanish).

[19] W.C. Park, A. Atreya, H.R. Baum, Experimental and theoretical investigation of heat and mass transfer processes during wood pyrolysis, Combust. Flame 157 (3) (2010) 481–494, http://dx.doi.org/10.1016/j.combustflame.2009.10.006.

[20] E. Pastor, L. Zárate, E. Planas, J. Arnaldos, Mathematical models and calculation systems for the study of wildland fire behaviour, Prog. Energy Combust. Sci. 29 (2) (2003) 139–153, http://dx.doi.org/10.1016/S0360-1285(03)00017-0.

[21] D. Prieto, M. Asensio, L. Ferragut, J. Cascón, Sensitivity analysis and parameter adjustment in a simplified physical wildland fire model, Adv. Eng. Softw. 90 (2015) 98–106, http://dx.doi.org/10.1016/j.advengsoft.2015.08.001.

[22] D. Prieto, M.I. Asensio, L. Ferragut, J.M. Cascón, A. Morillo, A GIS-based fire spread simulator integrating a simplified physical wildland fire model and a wind field model, Int. J. Geogr. Inf. Sci. 31 (11) (2017) 2142–2163, http://dx.doi.org/10.1080/13658816.2017.1334889.

[23] K. Radmanović, I. Dukić, S. Pervan, Specific heat capacity of wood, Drvna Industrija 65 (2) (2014) 151–157, http://dx.doi.org/10.5552/drind.2014.1333.

[24] R. Rothermel, A Mathematical Model for Predicting Fire Spread in Wildlands Fires, General Technical Report RMRS-GTR-115, U.S. Department of Agriculture, Forest Service, Rocky Mountain Research Station, 1972.

[25] A. Saltelli, M. Ratto, T. Andres, F. Campolongo, J. Cariboni, D. Gatelli, M. Saisana, S. Tarantola, Global Sensitivity Analysis. The Primer, John Wiley & Sons Ltd, 2008.

[26] A. Saltelli, S. Tarantola, F. Campolongo, M. Ratto, Sensitivity Analysis in Practice: A Guide to Assessing Scientific Models, John Wiley & Sons Ltd, 2004.

[27] A. Saltelli, S. Tarantola, K.P.-S. Chan, A quantitative model-independent method for global sensitivity analysis of model output, Technometrics 41 (1) (1999) 39–56, http://dx.doi.org/10.1080/00401706.1999.10485594.

[28] F. Sarrazin, F. Pianosi, T. Wagener, Global sensitivity analysis of environmental models: Convergence and validation, Environ. Model. Softw. 79 (2016) 135–152, http://dx.doi.org/10.1016/j.envsoft.2016.02.005.

[29] SIMLAB, Version 2.2. simulation environment for uncertainty and sensitivity analysis, 2009, Joint Research Centre of the European Commission.

[30] I. Sobol, Global sensitivity indices for nonlinear mathematical models and their Monte Carlo estimates, Math. Comput. Simulation 55 (1) (2001) 271–280, http://dx.doi.org/10.1016/S0378-4754(00)00270-6, The Second IMACS Seminar on Monte Carlo Methods.

[31] A. Sullivan, Wildland surface fire spread modelling, 1990–2007. 1: Physical and quasi-physical models, Int. J. Wildland Fire 18 (4) (2009) 349–368, http://dx.doi.org/10.1071/WF06143.

[32] A. Sullivan, Wildland surface fire spread modelling, 1990–2007. 2: Empirical and quasi-empirical models, Int. J. Wildland Fire 18 (4) (2009) 369–386, http://dx.doi.org/10.1071/WF06142.

[33] A. Sullivan, Wildland surface fire spread modelling, 1990–2007. 3: Simulation and mathematical analogue models, Int. J. Wildland Fire 18 (4) (2009) 387–403, http://dx.doi.org/10.1071/WF06144.

[34] S. Tarantola, W. Becker, Simlab software for uncertainty and sensitivity analysis, in: Handbook of Uncertainty Quantification, Springer, 2017, pp. 1979–1999, http://dx.doi.org/10.1007/978-3-319-12385-1_61.

[35] C. Tymstra, R. Bryce, B. Wotton, S. Taylor, O. Armitage, Development and Structure of Prometheus: the Canadian Wildland Fire Growth Simulation Model, Information Report NOR-X-417, Canadian Forest Service, Northern Forestry Centre, 2010.

[36] M. Vasconcelos, D. Guertin, FIREMAP - Simulation of fire growth with a geographic information system, Int. J. Wildland Fire 2 (2) (1992) 87–96, http://dx.doi.org/10.1071/WF9920087.

[37] X. Yang, M. Choi, G. Lin, G.E. Karniadakis, Adaptive ANOVA decomposition of stochastic incompressible and compressible flows, J. Comput. Phys. 231 (4) (2012) 1587–1614, http://dx.doi.org/10.1016/j.jcp.2011.10.028.